Effects of exposure of the leaf abaxial surface to direct solar radiation on the leaf anatomical traits and photosynthesis of soybean (*Glycine max* L.) in dryland farming systems

C. WANG[*], Y.M. DU[**], J.X. ZHANG[*], J.T. REN[*], P. HE[***], T. WEI[***], W. XIE[***], H.K. YANG[***,+] (iD), and J.X. ZHANG[*,+] (iD)

College of Agriculture, Xinjiang Agricultural University, Urumqi, 830052 Xinjiang, China[*]
Yili Institute of Agricultural Science, Yining, 835000 Xinjiang, China[**]
Key Laboratory of Crop Eco-Physiology & Farming System in Southwest China, Sichuan Agriculture University, 611130 Chengdu, Sichuan Province, China[***]

Abstract

The frequent occurrence of monsoon winds usually leads to the formation of inverted soybean leaves. However, the effect of leaf inversion on photosynthetic capacity remains unclear. The responses of leaf anatomical traits, chlorophyll fluorescence induction kinetics parameters, photosynthetic capacity, and nonstructural carbohydrates of fully expanded leaves to inversion of leaves in two soybean cultivars were studied. Leaf inversion decreased the stomatal size and thickness of developed leaves. The net photosynthetic rate was significantly reduced under leaf inversion, which resulted from reduced excitation energy trapping and electron transport of PSII reaction center. Leaf inversion increased leaf temperature 10 d after leaf inversion but reduced the instantaneous water-use efficiency compared to normally oriented leaves. Due to the decreased light-saturated net photosynthetic rate, the soluble sugars of light-sensitive cultivar decreased significantly. In summary, leaf inversion deactivated the PSII reaction centers, reduced photosynthesis and nonstructural carbohydrates in upper canopy soybean leaves.

Introduction

Soybean is a versatile crop grown worldwide. Soybean meal is the leading protein and energy source for human food and animal feed (Cai *et al.* 2020). Soybean is commonly grown in arid farming systems, accounting for 44% of China's total yield (Couée *et al.* 2006, Isoda *et al.* 2006). The frequent occurrence of monsoon winds

Highlights

- Leaf inversion leads to smaller stomata and thinner leaves
- Light-insensitive cultivar maintains T_{leaf} and P_N under leaf inversion
- Leaf inversion induced changes in the Chl *a* fluorescence kinetics OJIP curves

Abbreviations: ABS/RC – absorption flux per reaction center at t = 0; AQY – apparent quantum yield; Chl – chlorophyll; C_i – intercellular CO_2 concentration; E – transpiration rate; ET_0/CS – electron transport flux per cross-section at t = 0; ET_0/RC – electron transport flux per reaction center at t = 0; F_v/F_m – maximum quantum yield of PSII; g_s – stomatal conductance; LCP – light-compensation point; LSP – light-saturation point; PI_{abs} – performance index on absorption basis; PI_{total} – efficiency of energy conservation from absorbed photons to reduction of PSI end acceptors; P_N – net photosynthetic rate; P_{Nmax} – light-saturated net photosynthetic rate; RC/CS – relative number of active PSII reaction centers per excited cross-section; R_D – dark respiration rate; T_{leaf} – leaf temperature; TR_0/CS – trapped energy flux per cross-section at t = 0; TR_0/RC – trapped energy flux per reaction center at t = 0; WUE – water-use efficiency.

Conflict of interest: The authors declare that they have no conflict of interest.

usually leads to the inversion of soybean leaves, exposing the abaxial leaf surface to direct solar radiation, resulting in a decrease in plant photosynthesis (Zhang *et al.* 2016, Paradiso *et al.* 2020). Therefore, investigating the effect of leaf inversion on foliar anatomy traits and photosynthetic capacity will provide a theoretical basis for exploring a possible methodology for alleviating the decrease in plant photosynthesis caused by monsoon winds.

In soybean, solar radiation commonly strikes the adaxial leaf surface, and most of the chloroplasts are concentrated in the palisade tissue. The diffuse solar radiation, which reaches the leaf's abaxial surface, can enhance primary plant productivity, but it is less efficient under diffuse than direct light (Martin *et al.* 2009, Ichiro *et al.* 2016, Earles *et al.* 2017, Richardson *et al.* 2017, Paradiso *et al.* 2020). The leaf's abaxial surface usually receives 10% of the light intensity and the leaf inversion exposes the abaxial leaf surface to more potent solar radiation energy and broader spectra (Paradiso and Marcelis 2012, Paradiso *et al.* 2020). The abaxial and adaxial surfaces of leaves respond to high-energy direct solar radiation and lower-energy diffuse solar radiation varies in the light environment because of leaf anatomical traits (Paradiso and Marcelis 2012, Nazar *et al.* 2015, Pan and Guo 2016, Paradiso *et al.* 2020). The responses of photosynthesis and stomatal behaviors to the light intensity of the abaxial and adaxial sides have been reported in various plants (Soares-Cordeiro *et al.* 2011, Wang *et al.* 2011, Paradiso *et al.* 2020). Effect of simulated leaf inversion on foliar anatomical traits, photosynthesis, and nonstructural carbohydrates in soybean leaves remains unclear.

It is generally accepted that solar radiation is the most critical environmental factor affecting foliar anatomical traits and photosynthesis of leaves (Wu *et al.* 2017, Matthews *et al.* 2018, Yang *et al.* 2018). The most crucial stage for the accumulation of soybean storage components is the seed-filling stage (Chen *et al.* 2020) and the interaction between leaves and the light environment is fundamental for the energy balance of soybean plants (Tamagno *et al.* 2020). Leaf photosynthesis depends on gas exchange, CO_2 diffusion (Ellsworth *et al.* 2018), and carbon fixation (Ruiz-Vera *et al.* 2013). Leaf stomatal characteristics and the thickness of palisade tissue and sponge tissue constrained the evaporation, gas exchange, and CO_2 assimilation rate (Sefton *et al.* 2002, Terashima *et al.* 2011, Chen *et al.* 2015, Verboven *et al.* 2015, Flexas *et al.* 2018, Xiong *et al.* 2018, Lawson and Vialet-Chabrand 2019). The thicknesses of palisade and spongy tissues are strongly affected by light intensity (Bahamonde *et al.* 2018) and nitrogen and phosphorus contents (Li *et al.* 2017). Previous results have shown that thicker palisade tissues have higher photosynthetic efficiency (Chen *et al.* 2015). However, other studies have suggested that thicker leaves do not always accompany high photosynthetic capacity, owing to the efficiency of CO_2 diffusion from the air to the chloroplast (Earles *et al.* 2018, Flexas *et al.* 2018, Ellsworth *et al.* 2018) and adaptive strategies when plants are subjected to abiotic stress (Wu *et al.* 2017, Feng *et al.* 2019). Stomata are mainly distributed on the

abaxial surface and effective control of stomatal opening and closure significantly impacts leaf gas exchange, water balance, leaf temperature, and photosynthesis (Düring 2003, Voelker *et al.* 2016).

The abaxial surface of leaves is more susceptible to energetic solar radiation than the leaf adaxial surface because the stomata are mainly distributed on the abaxial surface (Li *et al.* 2010, Wang *et al.* 2020). When the abaxial surface of leaves is exposed to energetic solar radiation, the plant reduces the stomatal size and gas exchange actively to reduce leaf water loss. The light sensitivity of the abaxial surface of leaves cannot be entirely changed by an inversion treatment (Wang *et al.* 2011, Zhang *et al.* 2016). Solar radiation that reaches the leaf's abaxial surface causes irreversible reductions in plant photosynthesis and accumulation of seed-filling carbohydrates (Li *et al.* 2010). Previous studies have reported that leaf inversion reduces the effective regulation of stomatal opening and closure (Aasamaa and Aphalo 2017, Lawson and Vialet-Chabrand 2019), and thus affects the intercellular CO_2 concentration (C_i), leaf water loss, photosynthetic carbon fixation capacity, and the accumulation of plant biomass (Kromdijk *et al.* 2016). Notably, short-term leaf inversion reduces the net photosynthetic rate (P_N) by 20 to 30% (Turner and Singh 1984). In addition to these results, an exploration of how leaf inversion affects soybean photosynthesis is crucial for improving leaf photosynthesis in dryland farming systems.

The leaf's abaxial surface, which is exposed to direct solar radiation, naturally occurs as leaves sway because of monsoon winds. The application of leaf inversion to simulate the frequent occurrences of the effects of monsoon wind on leaf anatomical traits and photosynthesis capacity can provide a theoretical basis for exploring a possible methodology for alleviating the decrease in plant photosynthesis caused by monsoon winds. The present study aimed to investigate the responses of foliar anatomical traits, photosynthetic capacity, Chl fluorescence induction kinetics parameters, and nonstructural carbohydrates of fully expanded main stem leaves to light intensity and leaf inversion in two soybean cultivars with sensitivity to light intensity. We hypothesized that the frequent occurrence of monsoon winds leads to the inversion of soybean leaves at the grain-filling stage, which would reduce the gas exchange from the atmosphere to the primary sites of carbon fixation in the chloroplasts of soybean leaves.

Materials and methods

Experimental site: During the 2018 and 2019 cropping seasons, a field experiment was conducted at the experimental station (43°50'N, 80°04'E) of the Yili Institute of Agricultural Science, a typical dryland region in China. The annual accumulative rainfall for 2018 and 2019 was 226.1 and 203.2 mm, respectively. The experimental station's annual sun hours were 2,886.7 h, and the average solar radiation at noon was 2,100 μmol(photon) m^{-2} s^{-1} in 2019. The experimental site, located at mid-latitude westerlies, and the soybean in this growing area

frequently suffer from summer monsoon winds, leading to soybean leaf inversion, exposing the abaxial side of the leaf to the more energetic direct solar radiation [2,102 μmol(photon) m^{-2} s^{-1} at noon]. According to the Food and Agriculture Organization (FAO) soil taxonomy, the soil at the experimental site is a typical sandy loam. The root available soil N, P, and K contents were 54.8 g kg^{-1}, 17.3 g kg^{-1}, and 103.0 g kg^{-1}, respectively. The total N, P, and K were 0.4 mg kg^{-1}, 1.1 mg kg^{-1}, and 5.2 mg kg^{-1}, respectively. Soil N, P, and K contents were measured using the Kjeldahl digestion method, Bray method, and flame emission spectrophotometry, respectively (Yang *et al.* 2020).

Experimental design: Two widely grown soybean cultivars, Xindadou27 (XD27) and Jiyu60 (JY60), were used as experimental materials. These two soybean cultivars had similar plant heights (80–85 cm) and growth periods (110–115 d). In a historical set of cultivars, the photosynthetic rate (P_N) of JY60 decreased more rapidly in the leaf inversion treatment than in XD27. Therefore, JY60 is a light-sensitive cultivar that was introduced by the Heilongjiang Academy of Agricultural Sciences of China (45°58'N, 126°48'E). Xindadou27 is a light-insensitive cultivar that was released from the Xinjiang Agricultural University of China (43°57'N, 87°57'E). The split-plot experiment consisted of two treatment combinations with three replications each, two leaf inversion treatments as the main plot, and two light-sensitive cultivars as a subplot. Each plot was 4 m wide and 10 m long. For each treatment, 200 fully expanded leaves in the main stem were labeled with a tag at the seed-filling stage and fixed with a soft clip. These were labeled as the main plot, with the abaxial surface of the leaves exposed to direct solar radiation, while for the control group, regularly oriented fully expanded main stem leaves were used. Leaf inversion treatment was started from the soybean R5 stage to maturity. The labeled leaves were the fourth leaves from the top of the plant. The fourth leaf in the soybean plant received light intensity of 2,126 μmol(photon) m^{-2} s^{-1} of PPFD at noon. The leaf anatomical traits, photosynthetic capacity, and carbohydrate level responses to leaf inversion were determined. During the 2018 and 2019 cropping seasons, both XD27 and JY60 were sown on 11 April, with a density of 32.0 plants m^{-2}. The row spacing was 40 cm, and the plant spacing was 8 cm. A drip irrigation system was applied to irrigate each plot and the total amount of irrigation was 3,000 m^3 hm^{-2}. Nitrogen and phosphate were applied at the recommended rates of 144 kg(N) ha^{-1} and 103 kg(P$_2$O$_5$) ha^{-1}, respectively, using urea (46% N) and diamine phosphate (18% N and 46% P$_2$O$_5$). A total of 28.1% of N and all of the P were applied at sowing. The remaining N was applied at 103.5 kg(N) ha^{-1} by drip irrigation at the soybean R1 stage. Pest refers to local high-yielding practices.

Leaf anatomical structure: Leaf samples for both treatments were collected 10 d after the leaf inversion. The collected leaf samples were washed and fixed using a 50% formalin–acetic acid–alcohol (FAA) fixing liquid, consisting of 90% ethanol, 5% formaldehyde, and 5% glacial acetic acid, at 4°C for 1 d. The collected leaf samples were dehydrated with a graded series of ethanol (100, 95, 90, 80, 70, 60, and 50%) for 20 min. The dehydrated samples were dried using a freeze dryer instead of tertial-butanol. Field emission scanning electron microscopy (FESEM) of model *Zeiss SUPRA 55-VP* (Konigsallee, Germany) was used to scan the leaf cross-sections and abaxial surfaces of the collected leaf samples. The stomatal length, stomatal width, stomatal size, palisade tissue thickness, and spongy tissue thickness were quantified using *ImageJ* software (*Rawak Software Inc.*, Stuttgart, Germany).

Photosynthetic traits: The adaxial surface of fully expanded leaves in the main stem for both treatments were illuminated when they were inside the *CIRAS* chamber in both treatments. The P_N, transpiration rate (E), stomatal conductance (g_s), C_i, and instantaneous water-use efficiency (WUE) were measured from both treatments at 0, 2, 5, 10, 15, and 20 d after leaf inversion using a portable photosynthesis system (*CIRAS-3*, *PP Systems*, UK). Steady-state photosynthesis was achieved after the leaves were clamped for 5 min, and the photosynthetic parameters were recorded at 1,800 μmol(photon) m^{-2} s^{-1} light intensity, 400 ± 5 μmol mol^{-1} CO$_2$, and 70% humidity between 11:00–13:00 h (for details, *see* Wang *et al.* 2008). The instantaneous WUE was measured on the abaxial surface of leaves, and it was calculated using the following equation: WUE = P_N/E, where P_N is the net photosynthetic value and E represents the rate of leaf transpiration. The leaf temperature (T$_{leaf}$) was measured using an infrared thermometer (*DT8380*, *Anymetre*, China).

Photosynthetic light-response curves: Photosynthetic light-response curves of fully expanded leaves in the main stem of soybean were measured 10 d after leaf inversion using a portable photosynthesis system (*CIRAS-3*, *PP Systems*, London, UK) between 11:00–13:30 h at the soybean R5 expanding stage. The P_N was recorded at PPFDs of 2,000; 1,800; 1,500; 1,200; 1,000; 800, 600, 400, 200, 150, 100, 50, 30, and 0 μmol(photon) m^{-2} s^{-1}, respectively. These measurements were recorded at a fixed CO$_2$ concentration of 400 ± 5 μmol mol^{-1} using CO$_2$ cylinders. The photosynthetic light-response curves can be fitted with a nonlinear hyperbolic model (Farquhar *et al.* 2001), as follows:

$$P_N(I) = \frac{\alpha I + P_{Nmax} - \sqrt{(\alpha I + P_{Nmax})\alpha I + P_{Nmax} - 4\alpha I P_{Nmax}}}{2\theta} - R_D$$

where α is the apparent quantum yield (AQY), I represents the photosynthetic photon flux density (PPFD), P_{Nmax} is the maximum net photosynthetic rate, R_D is the dark respiration rate, and θ is the convexity. Linear regression analysis was performed using *SPSS version 19.0* software (*IBM*, Chicago, Illinois, USA) in the PPFD of 0 to 2,000 μmol(photon) m^{-2} s^{-1}. The crossover point of this line with the *x*-axis (photosynthetically active radiation, PAR) was the light-compensation point [LCP, μmol(photon)

m^{-2} s^{-1}], whereas the corresponding *x*-axis value for the crossover points along the *y*-axis was the light-saturation point [LSP, μmol(photon) m^{-2} s^{-1}].

The diurnal variation of the P_N and T_{leaf} were determined on three fully expanded main-stem leaves for each plot using a *CIRAS-3* Portable Photosynthesis System (*CIRAS-3, PP Systems*, UK) on bright days. The leaves were the fourth leaves from the top of the plant. Illumination was provided by sunlight, and the photosynthetic rate was recorded 15 d after treatment from 8:00–18:00 h, at 2-h intervals.

Fluorescence parameters: The rapid Chl *a* fluorescence induction kinetics of fourth fully expanded leaves were measured 10 d after treatments using a plant efficiency analyzer (*Pocket-PEA, Hansatech*, Norfolk, UK) between 11:00–13:00 h. After leaf samples for each treatment were acclimatized to the dark for 30 min using a fixing leaf clip, the samples were illuminated with a saturating light pulse of 3,000 μmol(photon) m^{-2} s^{-1} for 2 s, provided by an array of three light-emitting diodes (650 nm). The fast Chl *a* fluorescence kinetics was recorded from 10 μs to 1 s, the fluorescence intensity at 20 μs (F_O), 300 μs (F_K), and 2 ms (F_J) were collected, and all the collected data were analyzed using the program *PEA Plus* to obtain JIP-test parameters (Yusuf *et al.* 2010). These include F_v/F_m, maximum quantum yield of PSII; RC/CS, relative number of active PSII reaction centers per excited cross-section (CS); TR_0/CS, trapped energy flux per CS at t = 0; ET_0/CS, electron transport flux per CS at t = 0; ABS/RC, absorption flux per reaction center (RC) at t = 0; TR_0/RC, trapped energy flux per RC at t = 0; ET_0/RC, electron transport flux per RC at t = 0; PI_{abs}, performance index on absorption basis; PI_{total}, efficiency of energy conservation from absorbed photons to reduction of PSI end acceptors.

The Chl *a* fluorescence rise kinetics (OJIP) parameters were normalized between F_O and F_K expressed as V_{OK} [$V_{OK} = (F_t - F_O)/(F_K - F_O)$, 20–300 μs], and between F_O and F_J expressed as V_{OJ} [$V_{OJ} = (F_t - F_O)/(F_J - F_O)$, 20 μs to 2 ms]; finally, the differences between the transients expressed as ΔV_{OK} [$\Delta V_{OK} = V_{OK}$ (treatment) $- V_{OK}$ (control)] and ΔV_{OJ} [$\Delta V_{OJ} = V_{OJ}$ (treatment) $- V_{OJ}$ (control)] were determined to visualize the so-called L-band and K-band (Dalberto *et al.* 2017).

Chlorophyll (Chl) content: The leaves for both treatments were collected and freeze-dried to measure the contents of leaf Chl and soluble carbohydrates. Leaf Chl was extracted with ethanol and assessed spectrophotometrically following the method of Lichtenthaler (1987). The Chl *a*, Chl *b*, total Chl, and total carotenoids were calculated using following formulas: Chl a = 13.95 OD$_{665}$ − 6.88 OD$_{649}$, Chl b = 24.96 OD$_{649}$ − 7.32 OD$_{665}$, Car = (1,000 OD$_{470}$ − 2.05 Chl a − 114.8 Chl b)/245, Chl = Chl a + Chl b.

Nonstructural carbohydrates: The soluble sugars were extracted with 80% ethanol and quantified using the anthracene sulfuric acid method (Yang *et al.* 2017). In brief, 0.1 g of dried and powdered samples were extracted three times with 80% ethanol in a water bath at 80°C.

Measurements were recorded in a 96-well polystyrene plate using a *Benchmark* microplate reader (*Bio-Rad., Inc.*, California, USA) and quantified using glucose as a standard. The insoluble ethanol residue was used to extract the starch (Yang *et al.* 2017). The dried residue was kept in a boiling water bath for 15 min, and then hydrolyzed with 9.2 M HClO$_4$ for 15 min and extracted again using 2 mL of 4.6 M HClO$_4$ for 10 min. The supernatants were mixed, and the insoluble ethanol starch was measured spectrophotometrically at 620 nm using D-glucose as the standard.

Statistical analysis: All statistical data from the experiment were analyzed by two-way analysis of variance (*ANOVA*) using *SPSS version 19.0* (*SPSS Inc.*, Chicago, IL, USA). All data are presented as the mean ± standard error, and the means were compared using least significant difference (LSD) tests, *$P<0.05$, **$P<0.01$, in which the leaf inversion was set as the main plot, and the cultivars were set as the subplot. Graphs were plotted using *SigmaPlot* software *version 12.5* (*Systat Software, Inc.*, San Jose, California, USA). The contributions of each predictor variable to the decrease of P_N were analyzed by dominance analysis.

Results

Microstructure of soybean leaves: Microscopic observation of leaf cross-sections showed that leaf inversion significantly affected the palisade tissue of soybean leaves (Fig. 1, Table 1). The spongy mesophyll tissues of the leaf inversion treated plants were loosely attached, while the spongy mesophyll tissues of control plants were columnar, vertically oriented, and tightly packed. Microscopic
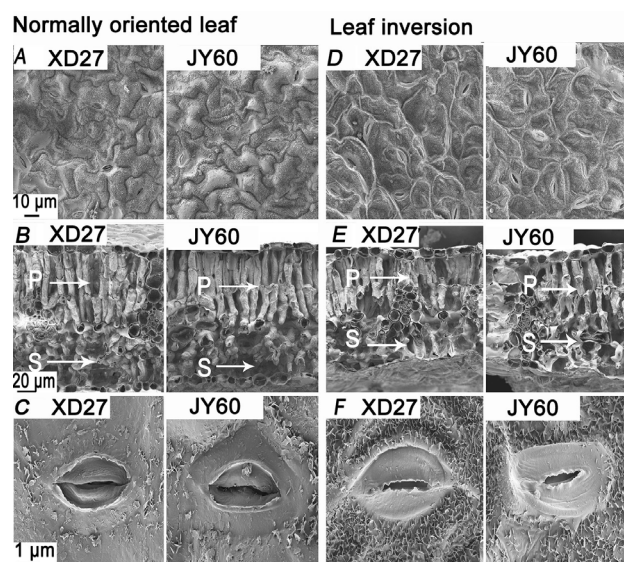

Fig. 1. The abaxial surface (*A,C,D,F*) and cross-sections (*B,E*) of the fourth main stem leaf for both leaf inversion and control plants for soybean cultivars XD27 and JY60: (*A–C*) represent normally-oriented leaves; and (*D–F*) represent the leaf inversion treatment. P – palisade tissue; S – spongy tissue.

observation of the leaf's abaxial surface showed a withered and wrinkled abaxial surface. The stomatal size was significantly lower than that of the control plants in 2018 and 2019.

The *ANOVA* showed that the leaf anatomical traits were significantly affected by leaf inversion, but not by the cultivar and their interactions (Table 1). Average leaf inversion treatments in the two growing seasons, the stomatal length, stomatal width, stomatal size, and thickness of the palisade and spongy tissues of XD27 were 13.3, 48.5, 42.7, 19.3, and 13.0% lower, respectively, than those of the control plants, and 16.9, 51.8, 31.9, 16.5, and 14.0% lower than those of the JY60 plants. However, there was no significant difference in stomatal density and the ratio of palisade and spongy tissue between the treatments for both cultivars.

Photosynthetic characteristics: Our results showed that the thicknesses of the palisade tissue and mesophyll cells were decreased by leaf inversion. Our experiments first

Table 1. Effects of leaf inversion on the leaf microstructure traits of soybean cultivars at 10 d after treatment. XD27 and JY60 represent soybean cultivars Xindadou27 and Jiyu60, respectively. PT/ST – the ratio of palisade tissue thickness to spongy tissue thickness. Data are expressed as means ± SE ($n = 6$). Values with *different letters* in a single column indicate a significant difference at $P<0.05$. ** indicates significant difference at the 0.01 probability level, and NS means nonsignificant difference ($P>0.05$).

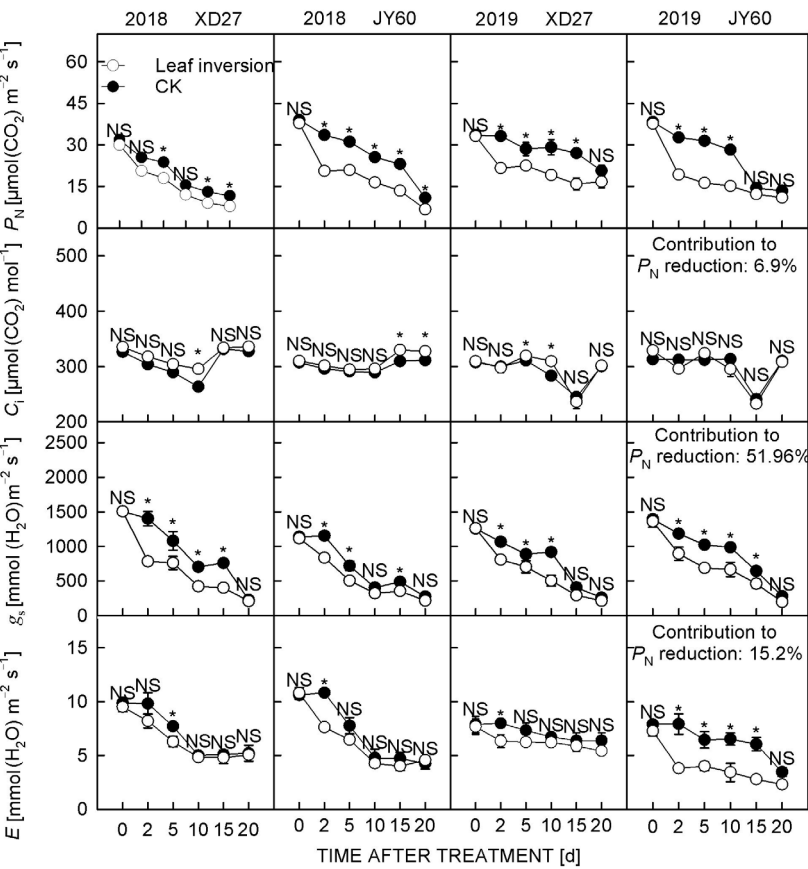| Cultivar	Treatments	Stomatal length [μm]	Stomatal width [μm]	Stomatal size [μm²]	Stomatal density [mm⁻²]	Palisade tissue thickness [μm]	Spongy tissue thickness [μm]	PT/ST
XD27	CK	12.70 ± 0.28ᵃ	4.93 ± 0.16ᵃ	43.65 ± 2.05ᵃ	243.50 ± 14.09ᵃ	114.28 ± 3.02ᵃ	83.37 ± 2.85ᵃ	1.40 ± 0.66ᵃ
	Leaf inversion	11.01 ± 0.47ᵇ	2.54 ± 0.29ᵇ	25.03 ± 2.76ᵇ	236.35 ± 25.15ᵃ	92.19 ± 1.33ᵇ	72.50 ± 2.76ᵇ	1.30 ± 0.54ᵃ
JY60	CK	12.84 ± 0.45ᵃ	5.10 ± 0.26ᵃ	41.56 ± 3.12ᵃ	214.32 ± 4.61ᵃ	111.08 ± 3.27ᵃ	84.31 ± 3.80ᵃ	1.35 ± 0.09ᵃ
	Leaf inversion	10.67 ± 0.62ᵇ	2.46 ± 0.36ᵇ	28.29 ± 1.87ᵇ	213.35 ± 8.82ᵃ	92.74 ± 1.76ᵇ	72.51 ± 3.94ᵇ	1.31 ± 0.08ᵃ
Source of variance								
Leaf inversion (T)		**	**	**	NS	**	**	NS
Cultivars (C)		NS	NS	NS	NS	NS	NS	NS
T × C		NS	NS	NS	NS	NS	NS	NS

Fig. 2. Effect of leaf inversion on the photosynthetic characteristics of soybean cultivars XD27 and JY60 in the 2018 and 2019 cropping seasons. Data are expressed as means ± SE ($n = 3$). P_N – net photosynthetic rate; C_i – intercellular CO_2 concentration; g_s – stomatal conductance; E – transpiration rate. * represents significant difference at the 0.05 probability level, and NS means nonsignificant difference ($P>0.05$).

measured the changes in the photosynthetic parameters of the two soybean cultivars (Fig. 2). The P_N of XD27 and JY60 was 22.3 and 29.3% lower in the leaf inversion treatments than that in the control plants. The g_s of the XD27 and JY60 plants were 24.6 and 21.2% lower, respectively, in the leaf inversion treatment than that in the control plants. However, there was no significant difference in the C_i and E, except for the E observed in JY60. The dominance analysis showed that the decreased g_s explained 52.0% of the total variation in P_N, followed by E (15.2%), WUE (13.3%), T_{leaf} (12.7%), and C_i (6.9%).

Diurnal pattern of net photosynthetic rate: The diurnal variation of P_N was observed 15 d after leaf inversion to investigate the influence of daily light intensities on the P_N of leaves (Fig 3). Based on the leaf inversion treatments in the two growing seasons, the average P_N values of XD27 and JY60 were 37.2 and 29.9%, respectively, which were lower in the leaf inversion treatments than that in the control plants. Notably, there was no significant difference between treatments at 8:00 h, and the maximum differences between treatments were observed from 10:00–14:00 h [2,095 μmol(photon) m^{-2} s^{-1}] for both cultivars (Fig. 3).

Instantaneous water-use efficiency: The WUE was calculated to clarify the leaf inversion effect on the stomatal water exchange of soybean leaves (Fig. 3). The WUE of XD27 decreased after leaf inversion, whereas the WUE of JY60 increased 10 d after treatment, with peak values of JY60 higher than XD27. Based on the leaf inversion treatments in the two cultivars, the average WUE observed 10 and 15 d after leaf inversion was 26.3 and 28.9%, respectively, which were lower than that in the control plants.

Leaf temperature: Given that leaf inversion leads to smaller stomatal dimensions and reduced WUE, our studies further investigated the daily T_{leaf} changes (Fig. 4). Averaging the leaf inversion treatments in the cropping seasons, the T_{leaf} of XD27 and JY60 in the leaf inversion treatments were 7.2 and 8.1% higher than that of the control group and there was no significant difference between the leaf inversion treatments at 0, 2, and 20 d after treatment. The daily variations in T_{leaf} showed significant differences between leaf inversion treatments at 10:00, 12:00, and 14:00 h. Averaged across years, the T_{leaf} of XD27 and JY60 were 4.8 and 6.8% higher than that of the control plants at 12:00 h.

The photosynthetic light-response curves were well-fitted by the rectangular hyperbolic model, as indicated by the coefficient of determination (R^2) values higher than 0.997 for both cultivars (Table 2, Fig. 5). The *ANOVA* showed that the P_{Nmax}, AQY, R_D, LCP, and LSP were significantly affected by leaf inversion, but not by the cultivar and their interactions. The P_{Nmax} of XD27 and JY60 decreased by 28.8 and 34.8%, respectively, compared with that of the control plants. The values of AQY in XD27 and JY60 decreased by 16.3 and 23.5%, respectively, compared with that of the control plants. The leaf inversion treatment decreased the LCP by an average of 18.1% for JY60 and
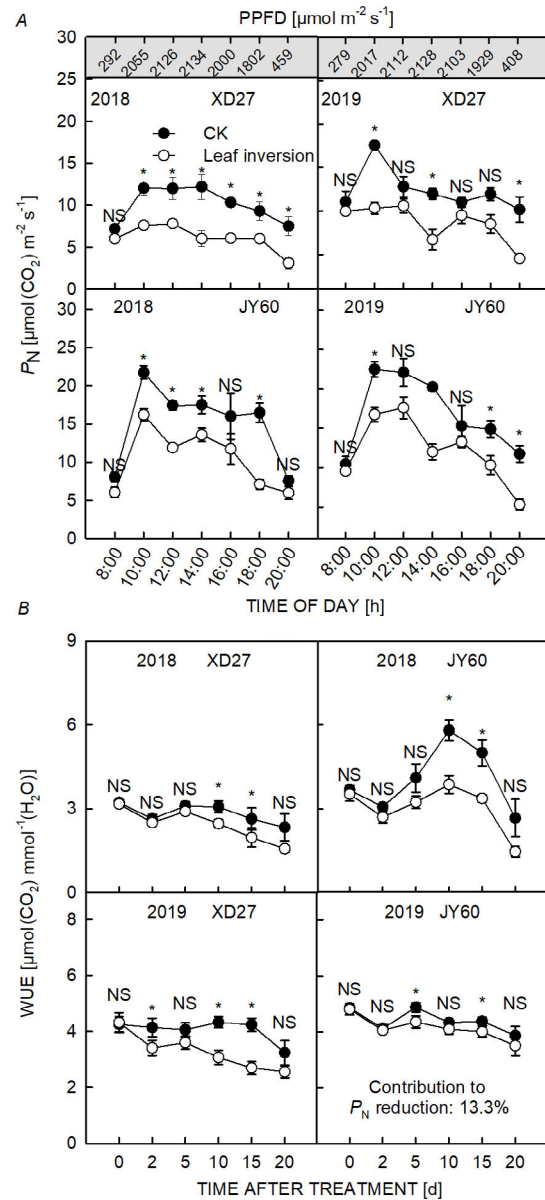

Fig. 3. Diurnal pattern of the net photosynthetic rate and instantaneous water-use efficiency (WUE) at 15 d after treatment in the 2018 and 2019 cropping seasons. XD27 and JY60 represent soybean cultivars, Xindadou27 and Jiyu60, respectively. Data are expressed as means ± SE ($n = 3$). * indicates significant difference at the 0.05 probability level, and NS means nonsignificant difference ($P>0.05$).

there was no significant difference observed for the LCP of XD27. The leaf inversion treatment decreased the LSP and the range of light-compensation point to light-saturation point (LCP–LSP) by averages of 14.2 and 14.7%.

Chl *a* fluorescence transient curves: Absorption per excited cross-section (ABS/CS), electron transport flux per reaction center (ET$_0$/RC), and maximum quantum yield of PSII (F_v/F_m) remained unchanged, but the electron
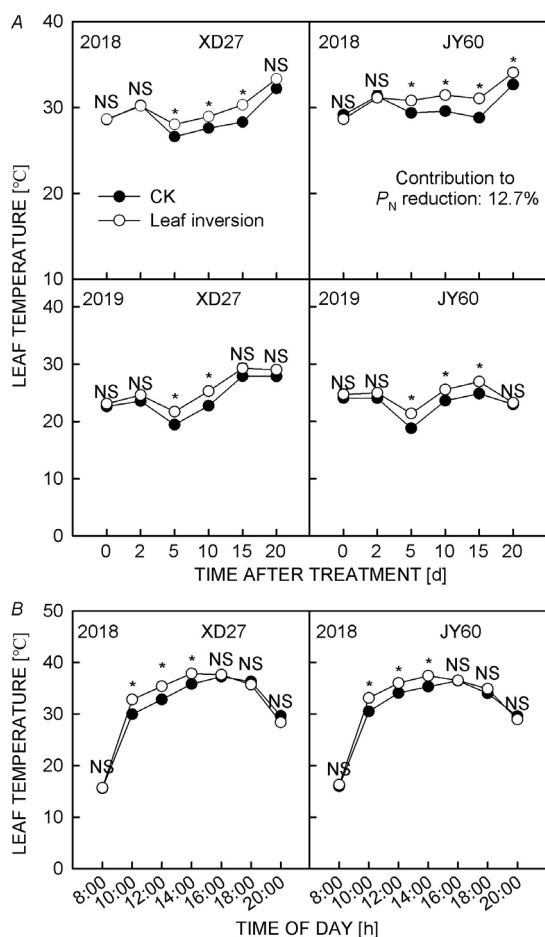
Fig. 4. Effect of leaf inversion on leaf temperature with days after treatment (*A*) and time of day (*B*) of XD27 and JY60. Data are expressed as means ± SE ($n = 3$). * indicates significant difference at the 0.05 probability level, and NS means nonsignificant difference ($P > 0.05$).

transport per excited cross-section (ET_0/CS) and active PSII reactions per excited cross-section (RC/CS) significantly decreased. For both cultivars, absorption flux (ABS/RC) and trapped energy flux per reaction center (TR_0/RC) significantly increased. Leaf inversion decreased the PI_{abs} and PI_{total} by 53.9 and 57.8%, respectively. The differential inductance curves of the O–K phase (ΔV_{OK}) and O–J phase (ΔV_{OJ}) indicated changes (0.076 rel. units) that occurred in 0.15 ms, and the ΔV_{OJ} indicated that changes (0.137 rel. units) occurred in 0.25 ms. The path analysis indicated that RC/CS (0.643) played a critical role in P_N reduction under leaf inversion.

Nonstructural carbohydrates and leaf Chl content: In cultivar JY60, leaf inversion resulted in significantly lower contents of Chl *a*, Chl *b*, total Chl, and carotenoid at 10, 15, and 20 d after leaf inversion, while there was no significant difference between the treatments in cultivar XD27 (Fig. 6). The average Chl *a*, Chl *b*, total Chl, and carotenoid contents of JY60 were 19.3, 19.1, 19.3, and 13.2% lower after the leaf inversion treatments than that in the control plants at 10, 15, and 20 d after treatment.

Leaf inversion reduced the soluble sugar and starch contents in the leaves of XD27 and JY60 at 20 d after leaf inversion (Fig. 6). In contrast, there were no significant differences between the treatments at 0 d after treatment. The average soluble sugars of XD27 and JY60 were 13.3 and 14.5%, respectively, lower in the leaf inversion treatments than that in the control plants at 20 d after leaf inversion. The average starch content of XD27 and JY60 in the leaf inversion treatments was 16.2 and 12.2%, respectively, lower than that of the control plants at 20 d after leaf inversion.

Discussion

Several studies have demonstrated that the contribution of the adaxial and abaxial surfaces of leaves to P_N varies with

Table 2. Photosynthetic light-response parameters of soybean leaves with leaf inversion and cultivars at 10 d after treatment. XD27 and JY60 represent soybean cultivars of Xindadou27 and Jiyu60. P_{Nmax} – maximum net photosynthetic rate; R_D – dark respiration rate; AQY – apparent quantum yield; LCP – light-compensation point; LSP – light-saturation point; LCP–LSP – the range of light-compensation point to light-saturation point. *Different letters* indicate a statistically significant level at $P < 0.05$. * and ** indicate significant difference at the 0.05 and 0.01 probability levels, respectively, and NS means nonsignificant difference ($P > 0.05$). Data are expressed as means ± SE ($n = 6$).

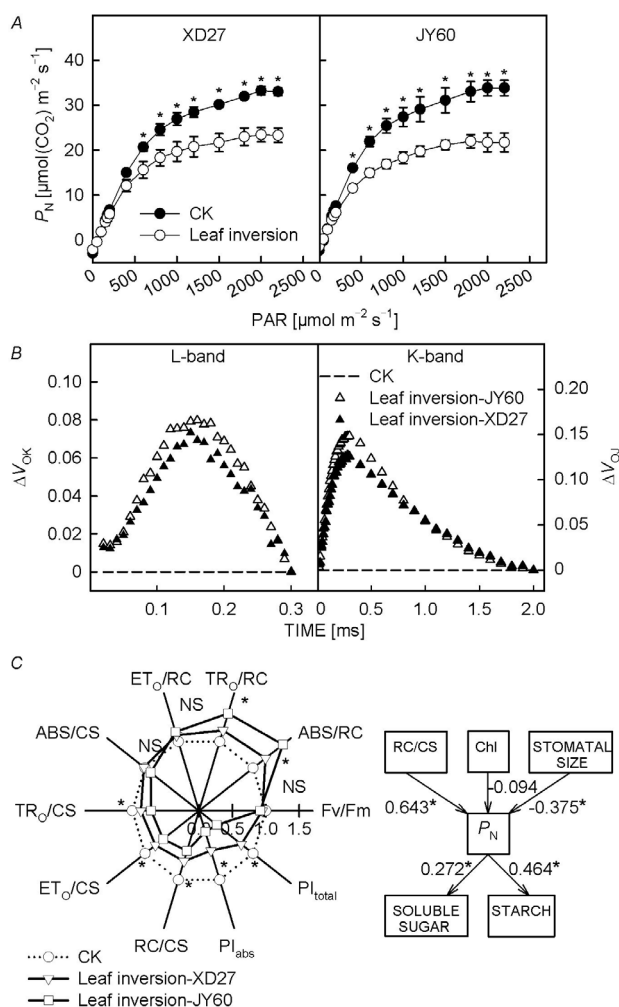| Cultivar	Treatment	P_{Nmax} [μmol(CO_2) m^{-2} s^{-1}]	R_D [μmol(CO_2) m^{-2} s^{-1}]	AQY [mol(CO_2) mol^{-1}(photon)]	LCP [μmol(CO_2) m^{-2} s^{-1}]	LSP [μmol(CO_2) m^{-2} s^{-1}]	LCP–LSP [μmol(CO_2) m^{-2} s^{-1}]
XD27	CK	41.3 ± 1.3[a]	3.2 ± 0.3[a]	0.049 ± 0.001[ab]	59.1 ± 2.3[a]	909.9 ± 43.2[a]	850.8 ± 47.5[a]
	Leaf inversion	29.4 ± 0.4[b]	2.5 ± 0.4[ab]	0.041 ± 0.003[bc]	56.5 ± 1.8[a]	786.5 ± 33.6[bc]	730.0 ± 53.5[bc]
JY60	CK	41.4 ± 1.3[a]	2.8 ± 0.3[a]	0.051 ± 0.002[a]	48.0 ± 1.7[b]	860.8 ± 16.1[ab]	812.9 ± 16.4[ab]
	Leaf inversion	27.0 ± 2.5[b]	1.7 ± 0.1[b]	0.039 ± 0.001[c]	39.3 ± 2.3[c]	732.3 ± 15.2[c]	693.0 ± 71.0[c]
Source of variance							
Treatment (T)		*	*	*	*	*	**
Cultivar (C)		NS	NS	NS	NS	NS	NS
T × C		NS	NS	NS	NS	NS	NS

Fig. 5. Net photosynthetic rate (P_N)–photosynthetically active radiation (PAR) response curves (*A*), Chl *a* fluorescence transient curves (*B*), and fluorescence parameters (*C*) for XD27 and JY60 under leaf inversion treatment in 2019. Chlorophyll *a* fluorescence transient curves normalized between F_O and F_K expressed as V_{OK} [$V_{OK} = (F_t - F_O)/(F_K - F_O)$], between F_O and F_J expressed as V_{OJ} [$V_{OJ} = (F_t - F_O)/(F_J - F_O)$]. $\Delta V_{OX} = V_{OX}$ (treatment) – V_{OX} (control). XD27 and JY60 represent soybean cultivars Xindadou27 and Jiyu60, respectively. F_v/F_m – maximum quantum yield of PSII; RC/CS – relative number of active PSII reaction centers per excited cross-section (CS); TR_0/CS – trapped energy flux per CS at $t = 0$; ET_0/CS – electron transport flux per CS at $t = 0$; ABS/RC – absorption flux per reaction center (RC) at $t = 0$; TR_0/RC – trapped energy flux per RC at $t = 0$; ET_0/RC – electron transport flux per RC at $t = 0$; PI_{abs} – performance index on absorption basis; PI_{total} – efficiency of energy conservation from absorbed photons to reduction of PSI end acceptors. * indicates significant difference at the 0.05 probability level, NS – not significant. Bars mean standard error (SE; $n = 3$).

growth conditions, genetic traits, and plant species (Martin *et al.* 2009, Soares-Cordeiro *et al.* 2011). Alternating adaxial, abaxial, and adaxial irradiation to simulate wind-induced leaf swaying has demonstrated that the abaxial surface of leaves exposed to direct solar radiation decreased

the P_N on both sides of the leaves (Zhang *et al.* 2016). In this study, leaf inversion significantly decreased P_N and g_s but not C_i and thus, one can conclude that stomatal closure is the primary reason for the reduced g_s. The reduced g_s in turn downregulated P_N which agrees with Pandey *et al.* (2007). Our view that changes in leaf anatomy determine photosynthesis reduction appears to agree with a previous study (Martin *et al.* 2009). The spongy mesophyll tissues are located on the abaxial side of the leaves, which are the active sites for gas exchange. The palisade mesophyll tissues are located on the adaxial surface of the leaves, which is the active site for light absorption (Evans 1999, Li *et al.* 2007). In this study, leaf inversion reduced stomatal size, stomatal density, palisade tissue, and spongy tissue thickness, partly explaining the decreased P_N in leaf inversion treatments. Similar results were also observed in trees and herbs (Zhang *et al.* 2016), suggesting that alternating adaxial and abaxial surfaces suppressed P_N. These results suggest that the leaf's abaxial surface is exposed more to direct solar radiation, which leads to thinner leaves, smaller stomata, and suppressed leaf photosynthesis. Thinner leaves have been reported to benefit CO_2 fixation by reducing the effective CO_2 path length (Terashima *et al.* 2006, Earles *et al.* 2018, 2019; Ellsworth *et al.* 2018), which is presumably not enough to compensate for the decreased leaf photosynthesis caused by leaf inversion. Further studies are required to determine the mesophyll conductance to CO_2 in leaf inversion treatments.

The stomatal response is a critical physiological adaptive mechanism that affects H_2O transport, heat transfer, and CO_2 diffusion, affecting the photosynthetic capacity and WUE of leaves (Fanourakis *et al.* 2016, Earles *et al.* 2019, Lawson and Vialet-Chabrand 2019, Harrison *et al.* 2020). Stomatal regulation often occurs after T_{leaf} increases, leading to the inhibition of CO_2 flux into the leaf when the abaxial surface is exposed to direct solar radiation. Stomatal responses to light intensity have been shown to vary depending on the genotype and environmental factors (Durand *et al.* 2020). Light intensity has a substantial stimulatory effect on cuticular permeability and stomatal closure because the stomata are mainly distributed on the abaxial surface of the leaf, and they are more sensitive to environmental changes (Soares-Cordeiro *et al.* 2011, Fanourakis *et al.* 2019). In this study, leaf inversion significantly reduced the stomatal size on the abaxial surface of leaves, which might be attributed to an active adaptation strategy, enabling plants to adapt to intense direct solar radiation and reduce excessive transpiration of leaves. Similar results were also observed in a previous study (Das *et al.* 2015).

The stomatal factor was the main reason for the decrease in P_N at a recoverable stress level, while it was considered that the nonstomatal limitations were the main reason for the decrease in P_N at the unrecoverable stress level (Yu *et al.* 2015, Hao *et al.* 2019). It was reported that salt, heavy metal, and osmotic stress induce significant changes in Chl *a* fluorescence rise kinetics, which elucidated significant alternations in PSII bioenergetics and many photosynthetic processes (Yusuf *et al.* 2010, Adamski *et al.*
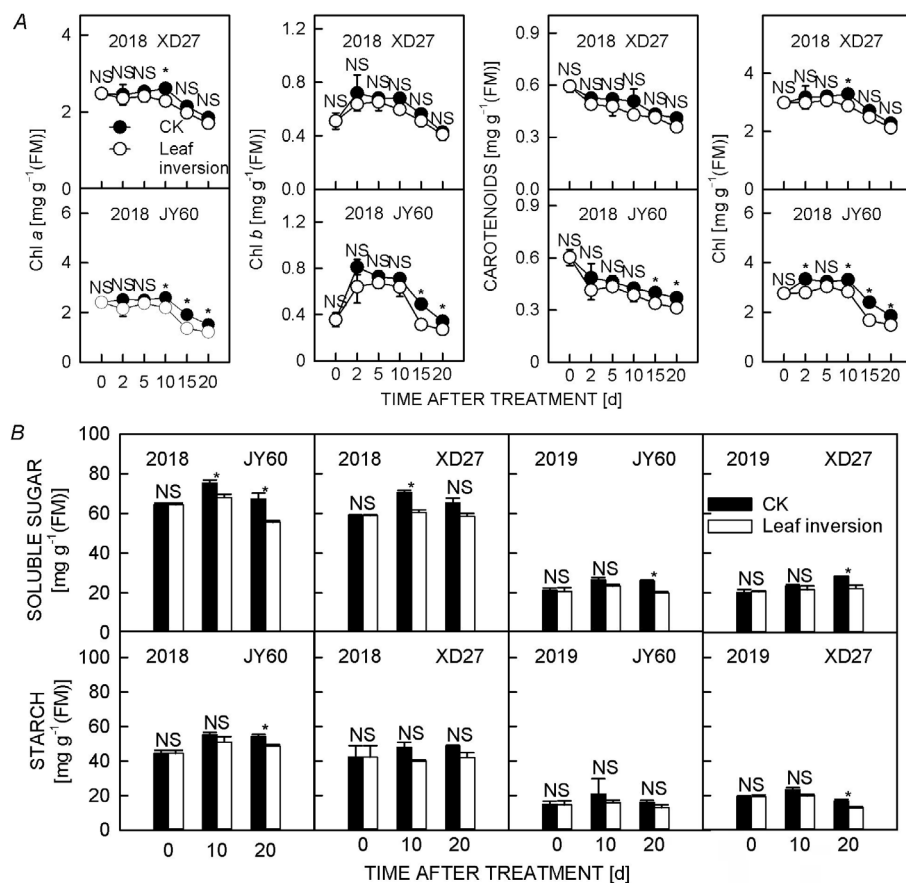
Fig. 6. Effects of leaf inversion on leaf chlorophyll, carotenoid, soluble sugar, and starch contents in leaves of XD27 and JY60. XD27 and JY60 represent soybean cultivars Xindadou27 and Jiyu60, respectively. Chl *a* – chlorophyll *a*; Chl *b* – chlorophyll *b*; Chl – chlorophyll. * indicates significant difference at the 0.05 probability level, and NS means nonsignificant difference ($P>0.05$). Bars mean standard error (SE; $n = 3$).

2011). In the present study, leaf inversion decreased PI_{abs} and PI_{total}, and both normalized L- and K-bands always showed positive curves, which indicated that leaf inversion decreased energy connectivity among PSII units and dissociation of the oxygen-evolving complex (Adamski *et al.* 2011). Thus, leaf inversion-decreased P_N mainly attributed to nonstomatal limitation because leaf inversion reduced electron transport (ET_0/CS) and excitation energy trapping (TR_0/CS), whereas leaf inversion did not affect intercellular CO_2 concentration (C_i). These findings suggest that the deactivation of PSII reaction center (RC/CS) might be the main reason for the P_N reduction under leaf inversion. Similar results have been reported for castor bean (*Ricinus communis* L.; Dalberto *et al.* 2017). The diurnal pattern of P_N showed a significantly lower peak value in the leaf inversion treatment, indicating that the abaxial surface of leaves, which were exposed to a more potent solar radiation energy and broader spectra, reduced the leaf photosynthetic capacity at noon (Fig. 5). Continuous leaf inversion led to an unrecoverable reduction in P_N at 10 d after leaf inversion, presumably due to decreased self-repair capability.

Leaf inversion led to an increase in the T_{leaf} by 7.2 and 8.1%, respectively, for the cultivars XD27 and JY60, compared with those of control plants (Fig. 4). In *Vicia faba* plants, the net assimilation rate achieved an optimum value when the T_{leaf} was 26–27°C (Avola *et al.* 2008). In this study, the average PAR and air temperature were

2,044.2 μmol(photon) m^{-2} s^{-1} and 37°C between 10:00–18:00 h at 0 d after treatment in two years, respectively. Leaf inversion treatments reduced the E of leaves, which was only observed for JY60 in 2019, partly explaining the increased T_{leaf}. Notably, the increased T_{leaf} for the soybean cultivar JY60 was higher than that of XD27, and the decreased E was only observed in JY60. These results suggest that the leaves of JY60 were more sensitive to direct solar radiation than that of XD27. This result might be because the abaxial surface of XD27 has a more robust capability of stomatal regulation to avoid excessive water loss by leaf transpiration. The leaf inversion treatment showed a significant photosynthetic break at 14:00 h, and the value of P_N was significantly lower than that of the control plants. We speculate that this might be attributed to the low light-saturation point of the abaxial side of the leaf, which agrees with the results in a study of rose plants (Paradiso and Marcelis 2012, Paradiso *et al.* 2020). These results suggest that leaf inversion increased the T_{leaf} at 5 and 10 d after treatment, and the light-insensitive cultivar XD27 has a more robust capability to maintain T_{leaf} under the leaf inversion treatment.

The P_N–PAR response curves of soybean leaves were fitted accurately using the rectangular hyperbolic model (Herrmann *et al.* 2020), as indicated by the R^2. Leaf inversion limited plant photosynthesis by decreasing P_{Nmax}, AQY, and LSP and decreasing the LCP–LSP, which agrees with previous results (Proietti and Palliotti

1997, Paradiso *et al.* 2020). The P_{Nmax} was significantly lower in all leaf inversion treatments, suggesting that leaf inversion decreased the potential photosynthetic capacity of soybean leaves. The AQY is an estimated value of the maximum efficiency of light congestion during CO_2 assimilation (Paradiso and Marcelis 2012). In this study, the AQY was significantly lower in the leaf inversion for the light-sensitive cultivar JY60 ($P<0.05$), but not for the light-insensitive cultivar XD27 ($P>0.05$), suggesting that leaf inversion decreased the utilization of solar radiation by soybean leaves. Additionally, the LSP and LCP–LSP of the inverted leaves were significantly reduced, suggesting that the potential of inverted leaves to use light energy was weakened. Dark respiration plays a pivotal role in carbon sequestration in environments that constrain variation in photosynthesis (Xu *et al.* 2013). In this study, the leaf inversion decreased R_D of light-sensitive cultivar JY60 but not light-insensitive cultivar XD27. The reduction of R_D was beneficial for the plant to maintain its metabolic balance by reducing the carbon loss of respiration under low solar radiation conditions. Similar adaptive strategies have also been observed under shading (Pires *et al.* 2011) and water stress (Xu *et al.* 2013). These results suggest that leaf inversion decreased the potential photosynthetic capacity of soybean leaves.

Numerous studies have reported that starch degradation in leaves is responsible for soluble sugar contents that protect plants against abiotic stress (Couée *et al.* 2006, Singh *et al.* 2015, Thalmann and Santelia 2017). In this study, both soluble sugar and starch contents decreased in the leaf inversion treatments at 20 d after leaf inversion for cultivar JY60, while there was no significant difference between the soluble sugar and starch content for treatments of the XD27 cultivar in 2018. These results can be attributed to the decreased P_N and the accumulation of starch in the leaves, which agrees with Iqbal *et al.* (2019). The decreased soluble sugar in our study might have resulted from the leaf inversion adaptation process. Sugars have been reported as signal molecules that protect cells from protein denaturation by protein–cell membrane hydrogen bonding during abiotic stress (Keunen *et al.* 2013). One possible reason is that the abaxial surface is usually adapted to the lower-energy diffuse solar radiation. The abaxial surface of leaves exposed to direct solar radiation caused by leaf inversion decreased the photosynthetic capacity of soybean leaves, which may be far greater than its self-repairing capability. Therefore, both soluble sugars and starch as energy sources decreased in the leaf inversion treatments at 20 d after leaf inversion.

Photosynthesis is a complex physiological process in which sunlight is converted into chemical energy in carbohydrates. Chl is an essential molecule in this process because it is the central pigment in photosynthesis. If its content is lowered, less solar energy is harvested, resulting in a decreased photosynthetic rate (Wen *et al.* 2011, Yan *et al.* 2015). In this study, when the abaxial surface was exposed to direct solar radiation, the Chl *a*, Chl *b*, total Chl, and carotenoid contents of JY60 decreased 10 d after treatment, while there was no significant difference between the Chl *a*, Chl *b*, total Chl, and carotenoid contents

of the treatments in the XD27 cultivar. The Chl content was closely related to P_N, which agrees with the results of Yao *et al.* (2017). The decreased P_N of JY60 in the main stem leaves treated with leaf inversion partly resulted from the decreased Chl content, which probably decreased the light energy conversion. Carotenoid content plays a vital role in protecting the photosynthetic apparatus from photooxidation damage (Demmig-Adams and Adams 1996). The decrease in carotenoid content in inverted leaves of JY60 aggravates the photooxidation damage of leaves under high light and high temperatures in summer.

The results of this study supported our hypothesis that the frequent occurrence of monsoon winds usually leads to inverted soybean leaves, which reduces gas exchange of leaves, and then reduces plant photosynthesis and nonstructural carbohydrates in soybean leaves. Further research may explore traits associated with mesophyll conductance to CO_2 in leaf inversion treatments for both cultivars. A recent study showed that the application of potassium, green leaf volatiles, and straw mulch-based no-tillage could protect plants against damage from abiotic stress by activating antioxidant enzymes and osmolyte accumulation (Singh *et al.* 2015, Cao *et al.* 2019, Tian *et al.* 2019, Yang *et al.* 2020). This study provides a theoretical basis for exploring a possible methodology for alleviating the decrease in plant photosynthesis under leaf inversion.

Conclusions: The abaxial surface of fully expanded leaves exposed to direct solar radiation decreased the P_N and P_{Nmax} by 25.8 and 32.0%, respectively, at the seed-filling stage, which can be attributed mainly to the deactivation of PSII reaction center (RC/CS). Leaf inversion leads to smaller stomata and thinner leaves, and the T_{leaf} increased by 7.6% at 10 d after leaf inversion, partly because of decreased E. The light-insensitive cultivar XD27 showed a higher capability to maintain T_{leaf}, WUE, AQY, soluble sugar, and chlorophyll under leaf inversion than the light-sensitive cultivar JY60. The AQY decreased in leaf inversion treatments, suggesting that leaf inversion decreased the potential photosynthetic capacity. Leaf inversion decreased the soluble sugar content of soybean leaves, suggesting that monsoon-induced leaf inversion reduced leaf photosynthesis, which might be attributed to decreased self-repairing capability after leaf inversion. This study provides a more comprehensive understanding of the effect of leaf inversion on leaf photosynthesis and the outputs of nonstructural carbohydrates. Future studies using green leaf volatiles, foliar potassium fertilizers, and straw mulching are required to explore a possible methodology for reducing the photosynthetic damage caused by monsoon-induced leaf inversion.

References

Aasamaa K., Aphalo P.J.: The acclimation of *Tilia cordata* stomatal opening in response to light, and stomatal anatomy to vegetational shade and its components. – Tree Physiol. **37**: 209-219, 2017.

Adamski J.M., Peters J.A., Danieloski R., Bacarin M.A.: Excess iron-induced changes in the photosynthetic characteristics of sweet potato. – J. Plant Physiol. **168**: 2056-2062, 2011.

Avola G., Cavallaro V., Patanè C., Giggi E.: Gas exchange and photosynthetic water use efficiency in response to light, CO_2 concentration and temperature in *Vicia faba*. – J. Plant Physiol. **165**: 796-804, 2008.

Bahamonde H.A., Gil L., Fernández V.: Surface properties and permeability to calcium chloride of *Fagus sylvatica* and *Quercus petraea* leaves of different canopy heights. – Front. Plant Sci. **9**: 494, 2018.

Cai Y.P., Wang L.W., Chen L. *et al*.: Mutagenesis of *GmFT2a* and *GmFT5a* mediated by CRISPR/Cas9 contributes for expanding the regional adaptability of soybean. – Plant Biotechnol. J. **18**: 298-309, 2020.

Cao Y., Ding W.W., Zhang J.Z. *et al*.: Significant down-regulation of urea cycle generates clinically relevant proteomic signature in hepatocellular carcinoma patients with macrovascular invasion. – J. Proteome Res. **18**: 2032-2044, 2019.

Chen B.B., Zhang G.Y., Li P.H. *et al*.: Multiple *GmWRI1s* are redundantly involved in seed filling and nodulation by regulating plastidic glycolysis, lipid biosynthesis and hormone signalling in soybean (*Glycine max*). – Plant Biotechnol. J. **18**: 155-171, 2020.

Chen B.Y., Wang C.H., Tian Y.K. *et al*.: Anatomical characteristics of young stems and mature leaves of dwarf pear. – Sci. Hortic.-Amsterdam **186**: 172-179, 2015.

Couée I., Sulmon C., Gouesbet G. *et al*.: Involvement of soluble sugars in reactive oxygen species balance and responses to oxidative stress in plants. – J. Exp. Bot. **57**: 449-459, 2006.

Dalberto D.S., Martinazzo E.G., Bacarin M.A.: Chlorophyll *a* fluorescence reveals adaptation strategies in drought stress in *Ricinus communis*. – Braz. J. Bot. **40**: 861-870, 2017.

Das R., Bhagawati K., Boro A. *et al*.: Relative performance of plant cultivars under respective water deficit adaptation strategies: A case study. – Curr. World Environ. **10**: 683-690, 2015.

Demmig-Adams B., Adams III W.W.: The role of xanthophyll cycle carotenoids in the protection of photosynthesis. – Trends Plant Sci. **1**: 21-26, 1996.

Durand M., Brendel O., Buré C., Le Thiec D.: Changes in irradiance and vapour pressure deficit under drought induce distinct stomatal dynamics between glasshouse and field grown poplars. – New Phytol. **227**: 392-406, 2020.

Düring H.: Stomatal and mesophyll conductances control CO_2 transfer to chloroplasts in leaves of grapevine (*Vitis vinifera* L.). – Vitis **42**: 65-68, 2003.

Earles J.M., Buckley T.N., Brodersen C.R. *et al*.: Embracing 3D complexity in leaf carbon–water exchange. – Trends Plant Sci. **24**: 15-24, 2019.

Earles J.M., Guillaume T., Roddy A.B. *et al*.: Beyond porosity: 3D leaf intercellular airspace traits that impact mesophyll conductance. – Plant Physiol. **178**: 148-162, 2018.

Earles J.M., Théroux-Rancourt G., Gilbert M.E. *et al*.: Excess diffuse light absorption in upper mesophyll limits CO_2 drawdown and depresses photosynthesis. – Plant Physiol. **174**: 1082-1096, 2017.

Ellsworth P.V., Ellsworth P.Z., Koteyeva N., Cousins A.B.: Cell wall properties in *Oryza sativa* influence mesophyll CO_2 conductance. – New Phytol. **219**: 66-76, 2018.

Evans J.R.: Leaf anatomy enables more equal access to light and CO_2 between chloroplasts. – New Phytol. **143**: 93-104, 1999.

Fanourakis D., Bouranis D., Giday H. *et al*.: Improving stomatal functioning at elevated growth air humidity: a review. – J. Plant Physiol. **207**: 51-60, 2016.

Fanourakis D., Hyldgaard B., Giday H. *et al*.: Stomatal anatomy and closing ability is affected by supplementary light intensity in rose (*Rosa hybrida* L.). – Hortic. Sci. **46**: 81-89, 2019.

Farquhar G.D., von Caemmerer S., Berry J.A.: Models of photosynthesis. – Plant Physiol. **125**: 42-45, 2001.

Feng L., Raza M.A., Li Z. *et al*.: The influence of light intensity and leaf movement on photosynthesis characteristics and carbon balance of soybean. – Front. Plant Sci. **9**: 1952, 2019.

Flexas J., Cano F.J., Carriquí M. *et al*.: CO_2 diffusion inside photosynthetic organs. – In: Adams III W.W., Terashima I. (ed.): The Leaf: A Platform for Performing Photosynthesis. Pp. 163-208. Springer, Cham 2018.

Hao L.H., Guo L.L., Li R.Q. *et al*.: Responses of photosynthesis to high temperature stress associated with changes in leaf structure and biochemistry of blueberry (*Vaccinium corymbosum* L.). – Sci. Hortic.-Amsterdam **246**: 251-264, 2019.

Harrison E.L., Arce Cubas L., Gray J.E., Hepworth C.: The influence of stomatal morphology and distribution on photosynthetic gas exchange. – Plant J. **101**: 768-779, 2020.

Herrmann H.A., Schwartz J.-M., Johnson G.N.: From empirical to theoretical models of light response curves-linking photosynthetic and metabolic acclimation. – Photosynth. Res. **145**: 5-14, 2020.

Ichiro T., Hiroki O., Takashi F., Riichi O.: Light environment within a leaf. II. Progress in the past one-third century. – J. Plant Res. **129**: 353-363, 2016.

Iqbal N., Hussain S., Raza M.A. *et al*.: Drought tolerance of soybean (*Glycine max* L. Merr.) by improved photosynthetic characteristics and an efficient antioxidant enzyme system under a split-root system. – Front. Physiol. **10**: 786, 2019.

Isoda A., Mori M., Matsumoto S. *et al*.: High yielding performance of soybean in northern Xinjiang, China. – Plant Prod. Sci. **9**: 401-407, 2006.

Keunen E., Peshev D., Vangronsveld J. *et al*.: Plant sugars are crucial players in the oxidative challenge during abiotic stress: extending the traditional concept. – Plant Cell Environ. **36**: 1242-1255, 2013.

Kromdijk J., Głowacka K., Leonelli L. *et al*.: Improving photosynthesis and crop productivity by accelerating recovery from photoprotection. – Science **354**: 857-861, 2016.

Lawson T., Vialet-Chabrand S.: Speedy stomata, photosynthesis and plant water use efficiency. – New Phytol. **221**: 93-98, 2019.

Li L., Shi Z.Y., Li L. *et al*.: Overexpression of *ACL1* (*abaxially curled leaf 1*) increased bulliform cells and induced abaxial curling of leaf blades in rice. – Mol. Plant **3**: 807-817, 2010.

Li P.M., Fang P., Wang W.B. *et al*.: The higher resistance to chilling stress in adaxial side of *Rumex* K-1 leaves is accompanied with higher photochemical and non-photochemical quenching. – Photosynthetica **45**: 496-502, 2007.

Li Q.L., Mao H.P., Zuo Z.Y. *et al*.: Effects of nitrogen and phosphorus on the microstructure and ultrastructure of tomato leaves (*Solanum lycopersicum*). – J. Plant Nutr. **40**: 1773-1783, 2017.

Lichtenthaler H.K.: Chlorophylls and carotenoids: pigments of photosynthetic biomembranes. – Method. Enzymol. **148**: 350-382, 1987.

Martin C.E., Hsu R., Lin T.C.: Comparative photosynthetic capacity of abaxial and adaxial leaf sides as related to exposure in two epiphytic ferns in a subtropical rainforest in Northeastern Taiwan. – Am. Fern J. **99**: 145-154, 2009.

Matthews J.S.A., Vialet-Chabrand S., Lawson T.: Acclimation to fluctuating light impacts the rapidity of response and diurnal rhythm of stomatal conductance. – Plant Physiol. **176**: 1939-1951, 2018.

Nazar R., Umar S., Khan N., Sareer O.: Salicylic acid supplementation improves photosynthesis and growth in mustard through changes in proline accumulation and ethylene formation under drought stress. – S. Afr. J. Bot. **98**: 84-94, 2015.

Pan J.Q., Guo B.L.: Effects of light intensity on the growth,

photosynthetic characteristics, and flavonoid content of *Epimedium pseudowushanense* BL Guo. – Molecules **21**: 1475, 2016.

Pandey R., Chacko P.M., Choudhary M. *et al.*: Higher than optimum temperature under CO_2 enrichment influences stomata anatomical characters in rose (*Rosa hybrida*). – Sci. Hortic.-Amsterdam **113**: 74-81, 2007.

Paradiso R., de Visser P.H.B., Arena C., Marcelis L.F.M.: Light response of photosynthesis and stomatal conductance of rose leaves in the canopy profile: the effect of lighting on the adaxial and the abaxial sides. – Funct. Plant Biol. **47**: 639-650, 2020.

Paradiso R., Marcelis L.F.M.: The effect of irradiating adaxial or abaxial side on photosynthesis of rose leaves. – Acta Hortic. **956**: 157-163, 2012.

Pires M.V., Almeida A.-A.F., Figueiredo A.L. *et al.*: Photosynthetic characteristics of ornamental passion flowers grown under different light intensities. – Photosynthetica **49**: 593-602, 2011.

Proietti P., Palliotti A.: Contribution of the adaxial and abaxial surfaces of olive leaves to photosynthesis. – Photosynthetica **33**: 63-69, 1997.

Richardson F., Brodribb T.J., Jordan G.J.: Amphistomatic leaf surfaces independently regulate gas exchange in response to variations in evaporative demand. – Tree Physiol. **37**: 869-878, 2017.

Ruiz-Vera U.M., Siebers M., Gray S.B. *et al.*: Global warming can negate the expected CO_2 stimulation in photosynthesis and productivity for soybean grown in the midwestern United States. – Plant Physiol. **162**: 410-423, 2013.

Sefton C.A., Montagu K., Atwell B.J., Conroy J.P.: Anatomical variation in juvenile eucalypt leaves accounts for differences in specific leaf area and CO_2 assimilation rates. – Aust. J. Bot. **50**: 301-310, 2002.

Singh M., Kumar J., Singh S. *et al.*: Roles of osmoprotectants in improving salinity and drought tolerance in plants: a review. – Rev. Environ. Sci. Biotechnol. **14**: 407-426, 2015.

Soares-Cordeiro A.S., Driscoll S.P., Arrabaça M.C., Foyer C.H.: Dorsoventral variations in dark chilling effects on photosynthesis and stomatal function in *Paspalum dilatatum* leaves. – J. Exp. Bot. **62**: 687-699, 2011.

Tamagno S., Sadras V.O., Ortez O.A., Ciampitti I.A.: Allometric analysis reveals enhanced reproductive allocation in historical set of soybean varieties. – Field Crop. Res. **248**: 107717, 2020.

Terashima I., Hanba Y.T., Tazoe Y. *et al.*: Irradiance and phenotype: comparative eco-development of sun and shade leaves in relation to photosynthetic CO_2 diffusion. – J. Exp. Bot. **57**: 343-354, 2006.

Terashima I., Hanba Y.T., Tholen D., Niinemets Ü.: Leaf functional anatomy in relation to photosynthesis. – Plant Physiol. **155**: 108-116, 2011.

Thalmann M., Santelia D.: Starch as a determinant of plant fitness under abiotic stress. – New Phytol. **214**: 943-951, 2017.

Tian S.F., Guo R.Z., Zou X.X. *et al.*: Priming with the green leaf volatile (Z)-3-hexeny-1-yl acetate enhances salinity stress tolerance in peanut (*Arachis hypogaea* L.) seedlings. – Front. Plant Sci. **10**: 785, 2019.

Turner N.C., Singh D.P.: Responses of adaxial and abaxial stomata to light and water deficits in sunflower and sorghum. – New Phytol. **96**: 187-195, 1984.

Verboven P., Herremans E., Helfen L. *et al.*: Synchrotron X-ray computed laminography of the three-dimensional anatomy of tomato leaves. – Plant J. **81**: 169-182, 2015.

Voelker S.L., Brooks J.R., Meinzer F.C. *et al.*: A dynamic leaf gas-exchange strategy is conserved in woody plants under changing ambient CO_2: evidence from carbon isotope discrimination in paleo and CO_2 enrichment studies. – Glob. Change Biol. **22**: 889-902, 2016.

Wang Y., Noguchi K., Terashima I.: Distinct light responses of the adaxial and abaxial stomata in intact leaves of *Helianthus annuus* L. – Plant Cell Environ. **31**: 1307-1316, 2008.

Wang Y., Noguchi K., Terashima I.: Photosynthesis-dependent and -independent responses of stomata to blue, red and green monochromatic light: differences between the normally oriented and inverted leaves of sunflower. – Plant Cell Physiol. **52**: 479-489, 2011.

Wang Z.T., Sun Z.Q., Lu S.: Optimal vegetation index for assessing leaf water potential using reflectance factors from the adaxial and abaxial surfaces. – Comput. Electron. Agr. **172**: 105337, 2020.

Wen K.J., Liang C.J., Wang L.H. *et al.*: Combined effects of lanthanumion and acid rain on growth, photosynthesis and chloroplast ultrastructure in soybean seedlings. – Chemosphere **84**: 601-608, 2011.

Wu Y.S., Gong W.Z., Yang W.Y.: Shade inhibits leaf size by controlling cell proliferation and enlargement in soybean. – Sci. Rep.-UK **7**: 9259, 2017.

Xiong D.L., Douthe C., Flexas J.: Differential coordination of stomatal conductance, mesophyll conductance, and leaf hydraulic conductance in response to changing light across species. – Plant Cell Environ. **41**: 436-450, 2018.

Xu W.Z., Deng X.P., Xu B.C: Effects of water stress and fertilization on leaf gas exchange and photosynthetic light-response curves of *Bothriochloa ischaemum* L. – Photosynthetica **51**: 603-612, 2013.

Yan Y.H., Wan Y., Liu W.G. *et al.*: Influence of seed treatment with uniconazole powder on soybean growth, photosynthesis, dry matter accumulation after flowering and yield in relay strip intercropping system. – Plant Prod. Sci. **18**: 295-301, 2015.

Yang F., Feng L.Y., Liu Q.L. *et al.*: Effect of interactions between light intensity and red-to-far-red ratio on the photosynthesis of soybean leaves under shade condition. – Environ. Exp. Bot. **150**: 79-87, 2018.

Yang H.K., Wu G., Mo P. *et al.*: The combined effects of maize straw mulch and no-tillage on grain yield and water and nitrogen use efficiency of dryland winter wheat (*Triticum aestivum* L.). – Soil Till. Res. **197**: 104485, 2020.

Yang H.K., Zhang X.Y., Chen B.L. *et al.*: Integrated management strategies increase cottonseed, oil and protein production: the key role of carbohydrate metabolism. – Front. Plant Sci. **8**: 48, 2017.

Yao X.D., Li C.H., Li S.Y. *et al.*: Effect of shade on leaf photosynthetic capacity, light-intercepting, electron transfer and energy distribution of soybeans. – Plant Growth Regul. **83**: 409-416, 2017.

Yu H.Y., Murchie E.H., González-Carranza Z.H. *et al.*: Decreased photosynthesis in the erect panicle 3 (ep3) mutant of rice is associated with reduced stomatal conductance and attenuated guard cell development. – J. Exp. Bot. **66**: 1543-1552, 2015.

Yusuf M.A., Kumar D., Rajwanshi R. *et al.*: Overexpression of γ-tocopherol methyl transferase gene in transgenic *Brassica juncea* plants alleviates abiotic stress: Physiological and chlorophyll *a* fluorescence measurements. – BBA-Bioenergetics **1797**: 1428-1438, 2010.

Zhang Z.S., Li Y.T., Gao H.Y. *et al.*: Characterization of photosynthetic gas exchange in leaves under simulated adaxial and abaxial surfaces alternant irradiation. – Sci. Rep.-UK **6**: 26963, 2016.